Heat exchange potential of energy tunnels for different internal airflow characteristics

Sarah C. Dornberger[1], Alessandro F. Rotta Loria[2,*],
Manlu Zhang[2], Leimin Bu[2], Jean-Luc Epard[1], and Pascal Turberg[3]

[1]University of Lausanne, Institute of Earth Sciences, Lausanne, CH
[*]Swiss Federal Institute of Technology in Lausanne, EPFL, Laboratory of Soil Mechanics, Lausanne, CH
[2]Northwestern University, Department of Civil and Environmental Engineering, Mechanics and Energy Laboratory, USA
[3]Swiss Federal Institute of Technology in Lausanne, EPFL, Civil Engineering Institute, Lausanne, CH
Corresponding author: af-rottaloria@northwestern.edu

Abstract

Energy tunnels allow the harvesting of untapped heat at shallow depths in the underground to meet the thermal energy requirements of buildings and infrastructures over large areas. Such heat can derive from two sources: the ground surrounding energy tunnels and the air circulating in the environment internal to these tunnels. To date, various investigations have addressed the role of ground characteristics on the heat exchange potential of energy tunnels, as they significantly influence the amount of geothermal energy that these geostructures can harvest. Despite the comparable role of airflow characteristics on the amount of aerothermal energy that energy tunnels can harvest, no extensive analysis of this problem has been reported before this study. To fill in this knowledge gap, this paper investigates the heat exchange potential of energy tunnels for a broad range of internal airflow characteristics. From this perspective, the work specifically provides: (i) the first charts, validated against representative experimental evidence, summarizing the thermal power that energy tunnels can harvest per unit surface for different convection heat transfer coefficients and temperatures associated with internal airflows, as well as undisturbed temperatures and effective thermal conductivities of the ground; and (ii) the analysis of an energy tunnel at the regional scale, based on the application of the developed charts and the use of a large hydrogeological dataset. Based on the results of this study, it is concluded that the internal airflow characteristics significantly influence the harvesting of aerothermal energy through energy tunnels. Together with the ground characteristics, which can markedly vary along energy tunnel applications at the regional scale, internal airflow characteristics rule the thermal power that can be harvested through such heat exchangers, deserving thorough quantifications for any adequate energy performance assessment.

Keywords: Energy tunnels, airflows, geothermal energy, aerothermal energy, charts, hydrogeology

1 Introduction

Technologies that can supply constructions with renewable thermal energy from the building to the district and city scales are of increasing interest to develop sustainable urban environments. Energy tunnels, among other energy geostructures, represent one of these technologies[1]. Similar to other relatively diffused energy geostructures, such as energy piles, energy tunnels transform conventional earth-contact structures into means to transfer untapped heat from the shallow subsurface to built environments for their heating and cooling, as well as the production of hot water. Different to other energy geostructures, such as energy piles, but similar to energy walls and slabs, energy tunnels not only allow the harvesting of shallow geothermal energy, but also aerothermal energy. This peculiarity results from the fact that energy tunnels present one interface with the ground and one interface with an internal environment wherein air typically flows, in contrast to only one interface with the ground that characterizes most energy geostructures and general shallow geothermal heat exchangers[2].

Design solutions, such as the pipe layout, critically influence the amount of heat that can be exchanged through energy tunnels[2,3], with the advantage that they can be tailored upon willingness for any site. The same consideration applies to other energy geostructures[4–8]. Site features, such as the ground and internal airflow characteristics, also play an equally important role in the heat exchange potential, with the main limitation that they are typically fixed for any location (airflow conditions may actually be modified on purpose through the use of ventilation systems or likely vary over the lifetime of projects).

In the context of energy tunnels and other relevant energy geostructures, critical ground characteristics include: (i) the presence, significance, and direction of groundwater flow; (ii) the temperature differential between the heat carrier fluid circulating in the pipes and the ground; and (iii) the effective thermal conductivity of the ground. Critical characteristics of internal airflows include: (i) the presence and significance of the airflow; (ii) the temperature differential between the heat carrier fluid circulating in the pipes and the air circulating in the underground environment; and (iii) the potential presence of heat sources in the internal environment. The temperature differential between the heat carrier fluid and the relevant surrounding environment (i.e., the ground surrounding the tunnel or the internal space to the tunnel) governs the actual heat exchange potential for a given inlet temperature of the heat carrier fluid circulating in the pipes. The magnitude of the groundwater flow or airflow facilitates the transfer of heat by convection in addition to conduction, such an influence increasing for a higher velocity of the relevant fluid in motion (e.g., groundwater in the ground or air within the tunnel). The relative influence of the previous site characteristics on the exchanged heat is tightly interconnected.

To date, the generalized analysis of the heat exchange potential of energy tunnels has been primarily addressed with a focus on the ground characteristics[9–11]. This focus has yielded charts that can aid the preliminary quantification of the thermal power per unit surface of energy tunnels in many

of the conditions that are likely to be encountered in practice[9]. The influence of the internal airflow characteristics on the heat exchange of energy tunnels has also been addressed in some studies[10,12,13], but always considering specific site conditions. No charts depicting the influence of varying internal airflow characteristics on the heat exchange potential of energy tunnels have been presented. Even for other energy geostructures, such as energy walls, the heat exchange potential has been primarily expanded considering the ground characteristics[8,14,15], yielding generalized charts[14,15]. Even in this case, studies have addressed the heat exchange between these energy geostructures and the internal underground environment[16,17], but only considering specific site conditions. In other words, no studies before the present one investigated the influence of the various internal airflow characteristics that are likely to be encountered in practice on the heat exchange potential of energy tunnels (and other energy geostructures presenting an interface with an internal underground environment). Yet, no charts were proposed to summarize the general influence of internal airflow characteristics on the heat exchange potential of energy tunnels.

Looking at the previous knowledge gap, this paper investigates the heat exchange potential of energy tunnels for a broad range of internal airflow characteristics. The present work specifically provides two contributions: (i) via three-dimensional, time-dependent, thermo-hydraulic, finite element simulations, the first experimentally validated charts summarizing the thermal power that energy tunnels can extract or inject per unit surface, depending on the convection heat transfer coefficient and temperature of internal airflows, for different undisturbed ground temperatures and effective thermal conductivities; and (ii) via the application of the charts and the consideration of a large hydrogeological and thermophysical dataset, partly gathered through experimental laboratory tests, the analysis of the heat exchange potential of an energy tunnel at the regional scale.

In the following, the charts summarizing the influence of internal airflow characteristics on the heat that can be exchanged through energy tunnels are presented and validated against the limited yet representative experimental evidence currently available. Next, the heat exchange potential of an energy tunnel at the regional scale is investigated. Then, a discussion of the obtained results is presented. Finally, concluding remarks that can be drawn from this work are reported.

2 Heat exchange potential charts for different internal airflow characteristics

2.1 General

This section quantifies the influence of different internal airflow characteristics on the thermal power that can be harvested per square meter of thermally active surface of energy tunnels. Three-dimensional (3-D), time-dependent, thermo-hydraulic, finite element simulations are performed to investigate:

- Energy tunnels that present internal airflows associated with different values of convection heat transfer coefficient (a proxy of the airflow velocity) and temperature. Such an approach allows addressing the heat exchange potential of energy tunnels in which natural or forced ventilations may be present, as well as wherein "hot" or "cold" airflows may occur. Considering the two variables mentioned above is critical for two reasons. First, because the velocity of airflows strongly influences the contribution of convection heat transfer in the global heat exchange process characterizing energy tunnels, and thus the relative significance of aerothermal and geothermal energy that is harvested through such energy geostructures. Second, because the temperature level of airflows strongly characterizes the efficiency and feasibility of using energy tunnels to provide heating or cooling (the cooling or heating of buildings may be inadequate or even infeasible when the temperature of internal airflows would be excessively high or low, respectively).
- Energy tunnels that are embedded by uniform geological formations of different values of effective thermal conductivity and undisturbed temperature. Such an approach allows addressing the heat exchange potential of energy tunnels constructed in dry and saturated geological formations, as well as located in cold, temperate and hot regions.

By accounting for the previous variables in sensitivity analyses, charts providing the thermal power per unit surface of energy tunnels under steady thermal conditions, which provide lower bound quantities for practical purposes[1], are developed. The rationale of the proposed charts is to help assess the heat exchange potential of energy tunnels in many practical situations without the expense of numerical simulations. The considered charts may also be employed to assess, through companion analytical calculations, the variation in the harvested thermal power through energy tunnels in situations where the internal airflow characteristics may change over the lifetime of such applications (e.g., when dealing with variations in airflow velocities or air temperatures caused by possible traffic blockages in the tunnel, lighting appliances, seasonal weather changes, and different intensities of combustion associated with running vehicles).

2.2 Numerical model

The energy tunnels numerically simulated in this study refer to an optimized design configuration by Cousin et al.[2] for one tunnel segmental lining. The considered energy tunnels have an outer diameter of $D_{out} = 9.50$ m and an inner diameter of $D_{in} = 8.70$ m. They are excavated at a depth that involves insensitivity to the thermal conditions characterizing the ground surface (i.e., depth of 19.7 m). Assumed infinitely long in extent, these energy tunnel segmental linings are composed of 2-m wide and 40 cm-thick rings. Each ring is constituted by six 4.20 m-long rectangular segments and one 3.40 m-long rectangular key, hosting a pipe layout perpendicular to the tunnel axis. The pipes are characterized by an inter-axis of 200 mm, an external diameter of 20 mm, a wall thickness of 1.9 mm,

and a normalized embedment of $s_i/t_l = 0.63$, where s_i is the distance from the tunnel intrados and t_l is the lining thickness.

The mathematical formulation employed for the present numerical analyses is detailed by Cousin et al.[2], among others[10,17–19]. From a qualitative perspective, these analyses simulate the operation of energy tunnels by accounting for the following heat transfer modes: conduction in the ground and the reinforced concrete that constitutes such energy geostructures; convection and conduction in the pipes; and convection with the internal underground built environment, which is reproduced by using an appropriate boundary condition at the interface between the tunnel and the internal environment (i.e., the actual fluid dynamics occurring in such environment is not modeled).

The finite element model that is used to reproduce one of the rings constituting the energy tunnels investigated in this study is reported in Fig. 1. The geometry of the considered model differs from the one analyzed by Cousin et al.[2] in that the modeled ring is embedded in a uniform geological formation instead of a stratified formation, and an optimized pipe configuration and embedment are employed (i.e., configuration 2.2 as described in the referenced work). Numerical results not presented here show that accounting for a uniform geological formation with average equivalent thermophysical properties to those considered by Cousin et al.[2] (i.e., thermal conductivity, density and specific heat of the various encountered layers down to the lower marl included) provides with a thermal power harvested through the same energy tunnels differing by less than 1%. For conditions in which the heat exchange in the ground is governed by conduction, it is in fact recognized that the *amount* of exchanged heat by energy geostructures primarily depends on an "effective" (average) value of thermal conductivity that characterizes the lithological units involved in the heat exchange process, rather than by the individual values of thermal conductivity[1]. Only the *spatial diffusion* of heat around energy geostructures depends on the specific values of the thermal conductivity characterizing different lithological units. The modeling of energy geostructures in uniform geological formations can thus be considered an effective approach to provide representative results of non-uniform geological formations. This consideration appears particularly valid when the difference between the properties of the lithological units does not change too abruptly from one layer to another. While no thermal interactions with the boundaries of the model were observed in this study over time, and a model with a tunnel located in its center would have provided the same results, considering the specific position of the tunnel reported by Cousin et al.[2] appeared relevant for consistency. Such a model is constituted by 393,083 domain elements, 18,788 boundary elements, and 3948 edge elements.

Based on the previous considerations, sensitivity analyses are run for addressing in a simplified manner the thermal power that can be harvested through energy tunnels embedded in a variety of geological formations with different equivalent thermophysical properties (specifically, effective

thermal conductivity). The obtained results thus inform charts that can be considered of broad applicability for preliminary energy analyses and designs of energy tunnels.

2.3 Initial and boundary conditions

In the numerical simulations, the initial temperature that characterizes the modeled ring and the surrounding ground is fixed to a constant value with depth of $T_0 \equiv T_{soil}$. Numerical results not reported in this work show that the consideration of a linearly increasing temperature with depth from the value of T_{soil} at the ground surface, following a geothermal gradient of 3°C per 100 m of depth, provides results that are up to 1% different from those reported here for the broad ranges of parameters considered. This result highlights the suitability of assuming a constant temperature field with depth, representative of the specific depth at which the tunnel is located, when the natural geothermal gradient is considered as the only potential perturbation of the ground temperature field. The same initial temperature $T_0 \equiv T_{soil}$ characterizes the water that serves as a heat carrier fluid within the pipes of the ring (modeling of the pipes is achieved through finite elements as described by Cousin et al[2], among others[10,17–19], and accounts for the heat conductance characterizing the heat transfer across the pipes). This water is initially considered immobile. To reproduce ground conditions that can be considered representative of cold, temperate and warm climates, numerical sensitivity analyses are run for varying values of $T_{soil} = 10$, 15, 20 and 25°C.

The modeling of infinitely long energy tunnel segmental linings is achieved by considering a symmetry plane on the two vertical boundaries of the numerical model that delimit the single ring. The temperature of the ground at the far-field boundaries (vertical and horizontal) is fixed to $T_\infty = T_{soil}$. A convection boundary condition is applied to the inner surface of the modeled ring by setting relevant values of the convection heat transfer coefficient h_c and air temperature $\bar{T}_a$. To reproduce internal conditions that can represent the absence of airflows or increasingly significant airflows associated with service tunnels, low-speed transport tunnels, and high-speed transport tunnels, numerical sensitivity analyses are run for varying values of $h_c = 0$, 2.5, 12.5 and 25 W/(m^2°C), respectively. These values of the convection heat transfer coefficient correspond to airflow velocities within tunnels with smooth internal surfaces of $\bar{v}_a = 0$, 0.3, 2.8 and 5.9 m/s, according to the correlations proposed by Peltier et al.[12] (in contrast to what would be predicted by the reference formulation, it is considered that when $h_c = 0 \Longrightarrow \bar{v}_a = 0$). To reproduce tunnels characterized by cold, temperate, warm and hot airflows, numerical sensitivity analyses are run for varying values of $\bar{T}_a = 10$, 15, 20 and 25°C, respectively.

The heat exchange operation of the modeled energy tunnels is reproduced by simulating the circulation of water in the pipes with a constant inlet velocity $\bar{v}_{in}$ that corresponds to a Reynolds number of $Re = 9000$, and constant inlet temperature $\bar{T}_{in}$. The chosen inlet velocity optimizes the pumping power requirements for the considered tunnel geometry and the heat transfer achieved

through the circulation of the heat carrier fluid in the pipes under turbulent flow conditions (to be generally preferred to laminar flow conditions for most energy tunnel applications). To reproduce heat extraction and injection operations, numerical sensitivity analyses are run for different values of $\overline{T}_{in} =$ 2 and 33°C, respectively. These values of inlet temperature may be considered to represent the minimum and maximum ones that are likely to characterize heat extractions and injections targeted by energy geostructures, respectively, thus maximizing the theoretical heat exchange potential of the modeled energy tunnels. Meanwhile, the provided heat exchange potential of energy tunnels is assessed in terms of lower bound values of thermal power that are associated with steady thermal conditions, thus providing with conservative estimates of the thermal power that is likely to be achieved under the transient conditions associated with the daily operation of such heat exchangers. The considered inlet temperature values also provide, for the minimum and maximum considered values of $T_{soil} = \overline{T}_a = 10$ and 25°C, a symmetrical temperature range of $\overline{T}_{in} - T_{soil} = \overline{T}_{in} - \overline{T}_a = \mp$ 8 and 23°C, respectively.

2.4 Material properties

The material properties employed in the present numerical analyses are summarized in Table 1. Temperature-dependent thermophysical properties characterize the water circulating in the pipes of the energy tunnels, while temperature-independent properties characterize the reinforced concrete that constitutes the energy tunnel and the surrounding ground. To reproduce operations of energy tunnels in a broad range of geological formations wherein conduction governs the harvesting of geothermal energy, numerical sensitivity analyses are run for different effective thermal conductivities of the ground of $\lambda_{soil} = 1.5$, 2.0, 2.5 and 3 W/(m °C).

2.5 Summary of sensitivity analyses

In summary, numerical sensitivity analyses are run in this study to investigate the heat exchange potential of energy tunnels for varying characteristics of internal airflows reproduced through different convection heat transfer coefficients of $h_c = 0$, 2.5, 12.5 and 25 W/(m^2°C), and airflow temperatures of $\overline{T}_a = 10$, 15, 20 and 25°C. To maximize the generality of the obtained results, different geological formations are considered with undisturbed temperatures of $T_{soil} = 10$, 15, 20 and 25°C, and effective thermal conductivities of $\lambda_{soil} = 1.5$, 2.0, 2.5 and 3 W/(m °C). Both heat extraction and injection operations are simulated, with reference to the circulation of a heat carrier fluid in the pipes under turbulent conditions with a constant inlet temperature of $\overline{T}_{in} = 2$ and 33°C, respectively.

Based on the previous sensitivity analyses, charts summarizing absolute values of the thermal power that can be extracted and injected per unit surface of energy tunnels are reported in the following. The thermal power per unit surface is quantified numerically as

$$\dot{q}_i = \frac{\dot{Q}}{w_{ring}\,\pi\,D_{in}} \quad (1)$$

where w_{ring} is the ring width and $\dot{Q}$ is the harvested thermal power, which is determined as

$$\dot{Q} = \dot{m}_f c_{p,f}(\bar{T}_{out} - \bar{T}_{in}) \quad (2)$$

where $\dot{m}_f$ and $c_{p,f}$ are the mass flow rate and specific heat of the heat carrier fluid circulating in the pipes, respectively, and $\bar{T}_{out}$ corresponds to the outlet fluid temperatures. The term $\dot{m}_f$ is calculated considering a density of the heat carrier fluid, ρ_f, that refers to the average between $\bar{T}_{in}$ and $\bar{T}_{out}$.

Absolute values of thermal power obtained after 30 days of simulation, which correspond to steady (flux) thermal conditions within the energy tunnels (considered as the heat exchangers composed of reinforced concrete, polyethylene pipes and water circulating into them), constitute the charts proposed hereafter. The considered simulation time involves for the different cases simulated in this work a variation of thermal power that is, on average, lower than 0.5% for a further day of operation beyond the 30th day, allowing to consider the obtained results a lower bound for practical purposes.

2.6 Heat extraction charts

Fig. 2 shows the thermal power that can be extracted per unit surface of energy tunnels for varying internal airflow characteristics. Under heat extraction operations, the harvestable thermal power from energy tunnels increases for airflows characterized by higher values of temperature and convection heat transfer coefficient, i.e., warmer and faster airflows. For any combination of airflow temperature and convection heat transfer coefficient, higher values of undisturbed temperature and effective thermal conductivity of the ground result in more significant thermal powers. Specifically, a more considerable influence of the effective thermal conductivity of the ground is observed for more significant values of undisturbed ground temperature. The minimum and maximum calculated values of thermal power are 7 and 102 W/m^2, respectively. In other words, different internal airflow characteristics can involve an extractable thermal power per square meter that can vary by a factor of 15.

2.7 Heat injection charts

Fig. 3 shows the thermal power that can be injected per unit surface of energy tunnels for varying internal airflow characteristics. Under heat injection operations, the harvestable thermal power from energy tunnels increases for airflows characterized by lower values of temperature and higher values

of convection heat transfer coefficient, i.e., cooler and faster airflows. For any combination of airflow temperature and convection heat transfer coefficient, lower values of undisturbed temperature and higher values of effective thermal conductivity of the ground result in more significant thermal powers. Specifically, a more considerable influence of the effective thermal conductivity of the ground is observed for lower values of undisturbed ground temperature. The minimum and maximum calculated values of thermal power are 6 and 101 W/m^2, respectively. In other words, different internal airflow characteristics can involve an injectable thermal power per square meter that can vary by a factor of 17.

2.8 Experimental validation of the charts

This section presents an experimental validation of the charts developed as a part of this work. This validation is made against three case studies: the energy tunnels located in Jenbach and Katzenberg, tested under a heat extraction operation by Franzius and Pralle[20], and the energy tunnel located in Seocheon, tested under a heat injection operation by Lee et al.[21] These case studies were selected according to a twofold rationale: first, they were described in a manner that allowed their numerical simulation through a relatively accurate representation of the site conditions in which they were operating; second, they operated under conditions for which a negligible groundwater flow could be considered, as previously commented by Di Donna and Barla[9].

Table 2 summarizes the relevant parameters considered for the numerical simulations of the investigated experimental case studies. The same numerical model used as a part of this work was employed for simulating the considered case studies, such an approach aiming at testing the validity of the values of thermal power per unit surface provided by the developed simulations and charts for different energy tunnels. The temperature and effective thermal conductivity of the ground surrounding the considered tunnels were taken from the works of Franzius and Pralle[20] and Lee et al.[21], or from Di Donna and Barla[9] when not available in the referenced original works. In the works of Franzius and Pralle[20] and Lee et al.[21], no information was reported about the specific values of airflow velocity characterizing the investigated energy tunnels, which would have allowed to calculate the corresponding convection heat transfer coefficient. Meanwhile, Di Donna and Barla[9] considered minimal airflows in the simulations of such energy tunnels. Accordingly, the convection heat transfer coefficient was varied in the present simulations from $h_c = 0$ to 1 W/(m^2°C), such values representing very limited airflows within energy tunnels[16,12]. The values of inlet temperature and velocity of the heat carrier fluid were considered equal to those employed in this study, depending on whether heat extraction or injection operations were simulated. The rationale of this choice was again aimed at validating the values of thermal power per unit surface of tunnel that might have been obtained by interpolation from the charts presented in this work.

Fig. 4 provides the experimental validation of the thermal power per unit surface provided by the charts presented in this work. In all cases, the experimental values of thermal power lie in the predicted ranges under steady conditions (i.e., after 30 days of simulation). It is worth noting that the modeled tunnels differed in tunnel type, tunnel geometry, pipe configuration and operative conditions as compared to the energy tunnel simulated in this study. Nevertheless, comparable results are obtained. Such an achievement corroborates the suitability of the charts proposed in this work for predicting the thermo-hydraulic behavior and energy performance of general energy tunnels with reasonable accuracy, at least in situations characterized by limited values of airflow velocity, such as those reproduced in this validation. New experimental evidence (e.g., considering significant values of airflow velocity in the tunnels) will be invaluable the expand the present validation in the future.

3 Heat exchange potential of an energy tunnel serving the regional scale

3.1 General

This section applies the developed charts to the analysis of the heat exchange potential of a hypothetical energy tunnel application at the regional scale located in the Jura Mountains, Switzerland. Based on the large scale of the considered application, a hydrogeological and thermophysical characterization of the subsurface is carried out through experimental laboratory tests to serve the use of the developed charts. Specifically, two-dimensional cross-sections that summarize the geological, hydrological and thermophysical characteristics of the subsurface are developed in the form of models, and subsequently used with the heat exchange charts to analyze the potential of the investigated energy tunnel application. The details of this analysis are reported in the sequel.

3.2 The regional area of interest

The energy tunnel addressed in the following represents a hypothetical 12 km-long underground infrastructure connecting the cities of Neuchâtel and La Chaux-de-Fonds in Switzerland. The tunnel is characterized by the same geometry as the one considered for the development of the charts proposed in this study. The chosen geographical area is selected due to interest in the expected geological and tectonic complexity, the presence of geothermal energy consumers, the possibility to obtain soil and rock samples on-site, and the availability of existing documentation to characterize the considered area comprehensively.

The Swiss geological context is very heterogeneous: crystalline, metamorphic and sedimentary rocks are intermingled in the Alps, while sedimentary rocks are mainly encountered in the Molassic basin and the Jura region. The Jura Mountain region, in particular, presents a complex geological environment in which many thrust faults and fold structures are present due to tectonic forces having

created the Alpine mountain chain[22] (Fig. 5). These deep fold structures cause the considered energy tunnel to be crossed by a wide variety of lithological units.

3.3 Geological characterization of the area

A substantial amount of literature data was available to characterize the geology of the considered area. Specifically, the selected area has been intensively characterized through studies reported by Kiraly[23], Sommaruga[24] and MFR SA[25]. Features including structural geology, lithostratigraphy, hydrogeology and geotechnics have been addressed in such studies.

Indications of dip and dip direction as well as of the thickness of each lithostratigraphic unit characterizing the selected site was found in the 1:25'000 Geological Atlas[26]. Further information about the underground geometry of the soil and rock layers was deduced from the cross-sections provided by the TransRUN study[25]. The geometry at greater depths was mainly drawn according to interpretations of the Jura fold structures determined by Sommaruga[24].

Based on the previous information, a geological model with the primary lithologies embedding the tunnel was determined (Fig. 6). It can be noted that the considered energy tunnel crosses many different lithologies.

3.4 Hydrological characterization of the area

A literature survey was carried out to obtain information about the hydrology of the considered area. Regional permeability values[27] and assumptions on saturation state were assessed from the study of Kiraly[23]. The SITN databases[28] provided complementary information about the location of groundwater springs and regional permeability. Limestones were considered as aquifers under fully saturated conditions when located below the groundwater table. It was considered that marl and clay layers were of low permeability and that the Molasse layer served as a semi-permeable layer. Nevertheless, there was very scarce direct information (e.g., from boreholes) on the groundwater table level along with the considered profile and at these depths. Therefore, the water table was determined based on a series of assumptions considering the groundwater flow in two dimensions within this profile, neglecting possible effects in the horizontal direction perpendicular to the cross-section. Where natural groundwater springs were present at the ground surface, it was considered that they represented the level of the groundwater table in the considered free-surface aquifer.

All of the data mentioned above were used to establish the hydrogeological model reported in Fig. 7. This hydrogeological model shows the hydraulic properties of each geological layer and includes the saturation state of each lithology embedding the energy tunnel profile.

3.5 Thermophysical characterization of the area

Based on the established geological and hydrological models, determining the thermophysical characteristics and properties of the lithologies at the considered site was needed for applying the heat exchange potential charts. Experimental laboratory tests were carried out to determine the thermophysical properties of the considered lithologies. Rock samples were collected through a large number of quarries and outcrops in the region, located in correspondence or close to the cross-section of interest. Fifteen primary lithologies were selected and sampled, at least three replicas for each of these lithologies were considered, and several properties were analyzed. The collected samples were all classified as sedimentary rocks and included limestones, sandstones, siltstones, marls and shales.

Density was measured using the volume calculated by X-ray micro-computed tomography scans and the image interpretation thereof (using the Amira-Avizo 3D Software). Mass was determined using a scale to weigh the sample when dry (after 24 hours in an oven at a temperature of $T = 105$ °C) and when saturated (after creating a vacuum and saturating the samples with deionized water for a time of $t = 24$ hours). Dry and saturated density values were calculated knowing the mass and the volume. Thermal conductivity was measured using a Neotim FP2C apparatus. A minimum of five measurements was done for each replica to ensure repeatability. Thermal conductivity was measured in dry and saturated conditions after weighing the samples. Correlations available in the literature between thermal conductivity and density, thermal conductivity and porosity, and thermal conductivity and water content were used to validate the experimental methods employed[1].

Fig. 8 shows a summary of the obtained experimental results. As expected, thermal conductivity depends not only on the soil or rock type, but also on the saturation state and porosity. For each lithology, values for thermal conductivity are always lower under dry conditions (light grey box plot) compared to saturated conditions (dark grey box plots), and when porosity is lower. From the obtained results, evident variations in thermal conductivity and density can be observed for the fifteen lithologies. As a consequence, such lithologies cannot be considered as homogeneous layers. This may lead to locally different estimations of the heat exchange potential along the energy tunnel.

Based on the previous information, the thermophysical model shown in Fig. 9 was created. This model provides a visualization of the zones of thermal interest along the tunnel path, at least from the perspective of the ground characteristics. Associated with each lithostratigraphic unit, a value of ground temperature was assigned based on the natural geothermal gradient present in the considered area. The categorization of the thermal conductivity values given in the legend was done by taking the average value for this parameter per lithology in dry and saturated conditions, and ranking these results from high to low. Five categories were determined from this analysis approach. The hydrogeological models allowed estimating the degree of water saturation of the lithologies, thus instructing about the zones for which values of saturated or dry thermal conductivity were to be used in the thermophysical model.

3.6 Assessment of the heat exchange potential of the energy tunnel

Using the established geological, hydrological and thermophysical models, the extractable thermal power per square meter of the energy tunnel was estimated with the developed charts. Precisely, by considering for each tunnel section the corresponding value of effective thermal conductivity and temperature of the ground, and an internal air temperature equal to the average ground temperature of all sections, a thermal power per square meter was calculated by considering four situations for the internal airflow. The absence of any airflow, i.e., $h_{c1} = 0$ W/(m^2°C). The presence of a minimal airflow, i.e., $h_{c2} = 2.5$ W/(m^2°C). The presence of a noteworthy airflow associated with relatively low-speed transport, i.e., $h_{c3} = 12.5$ W/(m^2°C). The presence of a significant airflow associated with a high-speed transport, i.e., $h_{c4} = 25$ W/(m^2°C).

The results of these estimations are summarized in Fig. 10. These results provide the heat exchange potential of the considered energy tunnel (e.g., for space heating or hot water production) depending on the internal airflow characteristics, as well as the local geological, hydrological, and thermophysical characteristics of the subsurface. Through these results, preferential zones of thermal activation may be determined based on the heat exchange potential and the energy demand of buildings located at the ground surface. Among the various energy tunnel sections, for example, the Callovian Section 30 was characterized by the highest heat exchange potential, despite not having the highest effective thermal conductivity. This result is due to the fact that the considered tunnel section is characterized by the highest ground temperature (due to its remarkable depth) and the most significant temperature differential between the heat carrier fluid circulating in the pipes and the airflow circulating in the tunnel.

Based on the previous estimations, the total thermal power associated with the considered 12 km-long energy tunnel was calculated (Table 3). The value of total thermal power can be used to gain a better understanding of the number of equivalent households served by the present energy tunnel application, based on national statistics of the annual heating consumption per household in Switzerland. In recent years, Swiss households consumed 52 TWh for space heating and 9 TWh for hot water production during one year[29]. By considering the Swiss population[30] and the average number of inhabitants per household, it is estimated that from 1097 to 4957 households could be provided with heating depending on the internal airflow conditions to the present energy tunnel. Alternatively, from 6341 to 28645 households could be provided with hot water. Yet, from 935 to 4226 households could be provided with both heating and hot water. The above estimates are conservative in that they do not consider the contribution of heat pumps being used to enhance the energy output from the ground, as well as potential groundwater flows present in the considered region that may enhance the estimated values of thermal power. To evaluate the exploitability of the tunnel in this theoretical study, an analysis of the end-user location was conducted. Population is

459 principally located at each end of the tunnel, at La Chaux-de-Fonds to the north (37,472 inhabitants[31]),
460 Hauterive to the south (2,647 inhabitants[31]), as well as above the central segments of the tunnel, at
461 Val-de-Ruz district (17,009 inhabitants[31] spread out over a wider area than just above the tunnel
462 location). These areas are shown in Figure 5. Considering a "service zone" of 500 m in radius from
463 the tunnel track, the exploitability potential of the tunnel was estimated. Three zones of potential were
464 defined: (i) high exploitability potential, if densely inhabited areas (more than 250 people per square
465 kilometer) were located within a 500 m radius from the tunnel track, (ii) medium exploitability
466 potential, if less densely inhabited areas (less than 250 people per square kilometer) were located
467 further away from densely inhabited areas, but still within a 500 m radius from the tunnel track, and
468 (iii) low exploitability potential, if inhabited areas were located farther away than 500 m from the
469 tunnel track. These categories are reported in Figure 10 for different tunnel sections. Such an analysis
470 can be used to further determine where heat pumps could be installed at surface-level to obtain the
471 highest energy yield. Meanwhile, the preceding estimate is indeed preliminary and simplified, because
472 it does not include the precise spatial locations of the served households at the surface, the tunnel
473 depth relative to these locations, the temperature drops and the infrastructure related to the distribution
474 of the heat to such households, and the details of the legislative feasibility of such applications.
475 Developed considerations about these subjects have been reported elsewhere[32–35]. Detailed energy
476 analyses and designs of any energy tunnel should always be performed subsequently to feasibility
477 studies or schematic designs using heat exchange charts.
478

479 ## 4 Discussion

480 This study highlights the critical role of different internal airflow conditions on the heat exchange
481 potential of energy tunnels. The proposed charts specifically highlight that the two most significant
482 characteristics that govern the interplay between the operation of energy tunnels and the harvesting of
483 aerothermal energy are (i) the absolute temperature difference between the heat carrier fluid
484 circulating in the pipes and the air circulating in the internal underground environment, and (ii) the
485 presence and significance of airflows. This consideration is complementary to the critical role of the
486 temperature difference between the heat carrier fluid circulating in the pipes and the ground, and the
487 presence and significance of groundwater flows that have been highlighted for the harvesting of
488 geothermal energy through energy tunnels[9] and energy walls[14]. As a matter of fact, the heat exchange
489 potential of energy tunnels is contemporaneously governed by the characteristics of the ground and
490 the internal underground environment, which act as a series of thermal resistances that can facilitate
491 or hinder the heat transfer (e.g., depending on the significance of airflows and groundwater flows).
492 Indeed, the charts presented here should only be used for preliminary assessments of the heat
493 exchange potential of energy tunnels for different internal airflow characteristics, as they do not allow
494 to explicitly account for the time-dependence of all heat transfer phenomena. While these temperature

levels have been maximized for providing the highest initial theoretical heat transfer potential, reference to steady thermal conditions yields lower thermal powers than those that may be expected in actual operations of energy geostructures under transient conditions. Specifically, the provided values of thermal power under steady conditions may be considered representative of general energy tunnels designed to exploit the maximum temperature differential at the inlet and outlet of the pipes, rather than significant pumping powers for obtaining the same thermal power for a more limited temperature differential. Therefore, the obtained values of thermal power may be considered representative of reality and useful for assessing many practical site conditions (hot tunnels serving space heating and/or water production). The experimental validation of the charts reported in this work corroborates the aforementioned considerations. Meanwhile, dynamic 3-D numerical simulations should always be considered necessary for detailed analyses and designs of energy geostructures.

In the context of the heat exchange potential assessment of an energy tunnel at the regional scale, this study further highlights the enormous variability of the ground characteristics that can be encountered over large areas. This aspect makes the analysis of the heat exchange potential of energy tunnels more complex than other energy geostructures commonly applied in more localized areas (e.g., limited to the footprint of one building, such as in the case of energy piles, or in that of energy walls and slabs constituting small underground parking garages). The gathering of representative geological, hydrological and thermophysical information is essential in this context.

As highlighted in this study, local heterogeneities are frequently encountered in the subsurface. Literature data, as well as field and laboratory observations, are valuable for assessing these heterogeneities and minimizing prediction errors of the heat exchange potential. Nevertheless, the influence of local heterogeneities on the heat exchange potential could generally be considered less significant compared to the role played by the significance of airflows and groundwater flows.

Results not presented herein suggest that a variation of about $\pm 11\%$ in the total thermal power harvested from the considered tunnel can be achieved, if reference is made to the maximum or minimum values of thermal conductivity along the tunnel, for the internal airflow characteristics considered. This range is significant in terms of housing thermal power, although it also indicates that local lithological variations do not represent a sensitive source of error for heat exchange potential diagnoses at a regional scale. Consequently, it is not necessary to know with an extreme level of detail the thermophysical properties associated with different lithostratigraphic units for obtaining a representative estimate of the energy yield when considering a regional scale. Meanwhile, having detailed knowledge of local lithological variations allows identifying the most promising areas for subsurface energy harvesting as a function of the number of consumers located nearby and the local subsurface characteristics. Considering local thermal heterogeneities is particularly essential where uniformity of the underground characteristics cannot be presumed at the beginning of the study.

5 Concluding remarks

This study addressed the influence of varying internal airflow characteristics on the heat exchange potential of energy tunnels. For the first time, the present research provided charts summarizing the thermal power that can be extracted and injected per unit surface of energy tunnels for many different internal airflow characteristics, and applied these charts to the analysis of the heat exchange potential of an energy tunnel at the regional scale regarding hydrogeological and thermophysical data. The main conclusions that can be drawn from this work are as follows:

- Airflows govern the harvesting of aerothermal energy through energy tunnels in much the same way groundwater flows govern the harvesting of geothermal energy.
- The two most significant characteristics related to internal airflows that govern the harvesting of aerothermal energy from energy tunnels are (i) the absolute difference between the temperature of the heat carrier fluid circulating in the pipes and the temperature of the airflow, as well as (ii) the velocity of the airflow. This conclusion explicates the essence of Newton's law of cooling.
- Depending on the internal airflow characteristics, from about 10 to 100 W/m^2 of thermal power can be harvested per unit surface of energy tunnels. Values higher than 50 W/m^2 may be considered representative of markedly favorable site characteristics (e.g., due to significant hot or cold airflows for heat extraction and injection operations, respectively). In general, this result highlights the significant potential of energy tunnels to supply substantial amounts of thermal energy to built environments.
- When assessing the heat exchange potential of energy tunnels at the regional scale, knowledge of geological, hydrological, and thermophysical data is necessary to describe the ground characteristics surrounding such infrastructures in addition to the internal airflow characteristics. All of these characteristics equally contribute to the thermal energy that can be harvested through energy tunnels.
- The variability of the ground characteristics at the regional scale can be extremely significant, showing markedly different thermophysical properties for different lithological units crossed by energy tunnels. Nevertheless, representative estimates of the heat exchange potential of energy tunnels at the regional scale may be considered to primarily depend on the significance of the airflow characteristics, rather than the specific values of the thermophysical properties of the ground. The same consideration appears to apply to the role of the groundwater flow characteristics on the definition of the overall heat exchange potential of energy tunnels.

Acknowledgments

The authors wish to acknowledge the following people for contributing to the achievements of several results presented in this work. Christian Rieben (MFR SA), David Giorgis (VD), Christophe Dénervaud (NE), Christophe Veuve (Juracime SA) and Christophe Nussbaum (Swisstopo) are thanked for their advice and availability to grant access to sampling sites for the experimental part of this investigation. Laurent Gastaldo (EPFL) is greatly acknowledged for allowing the use of much of the equipment needed for the preparation and analysis of core samples. Lyesse Laloui (EPFL) and Gary Perrenoud (EPFL) are acknowledged for providing technical assistance with some complementary activities to this research.

References

1. Laloui, L. & Rotta Loria, A. F. *Analysis and Design of Energy Geostructures: Theoretical Essentials and Practical Application*. (Academic Press, 2019).
2. Cousin, B., Rotta Loria, A. F., Bourget, A., Rognon, F. & Laloui, L. Energy performance and economic feasibility of energy segmental linings for subway tunnels. *Tunn. Undergr. Space Technol.* **91,** 102997 (2019).
3. Barla, M. & Di Donna, A. Energy tunnels: concept and design aspects. *Undergr. Space* **3,** 268–276 (2018).
4. Loveridge, F. & Powrie, W. 2D thermal resistance of pile heat exchangers. *Geothermics* **50,** 122–135 (2014).
5. Batini, N., Rotta Loria, A. F., Conti, P., Testi, D., Grassi, W. & Laloui, L. Energy and geotechnical behaviour of energy piles for different design solutions. *Appl. Therm. Eng.* **86,** 199–213 (2015).
6. Di Donna, A., Cecinato, F., Loveridge, F. & Barla, M. Energy performance of diaphragm walls used as heat exchangers. *Proc. Inst. Civ. Eng.-Geotech. Eng.* **170,** 232–245 (2017).
7. Sterpi, D., Coletto, A. & Mauri, L. Investigation on the behaviour of a thermo-active diaphragm wall by thermo-mechanical analyses. *Geomech. Energy Environ.* **9,** 1–20 (2017).
8. Zannin, J., Ferrari, A., Pousse, M. & Laloui, L. Hydrothermal interactions in energy walls. *Undergr. Space* (2020). doi:https://doi.org/10.1016/j.undsp.2020.02.001
9. Di Donna, A. & Barla, M. The role of ground conditions on energy tunnels' heat exchange. *Environ. Geotech.* **3,** 214–224 (2016).
10. Bidarmaghz, A. & Narsilio, G. A. Heat exchange mechanisms in energy tunnel systems. *Geomech. Energy Environ.* **16,** 83–95 (2018).
11. Epting, J., Baralis, M., Künze, R., Mueller, M. H., Insana, A., Barla, M. & Huggenberger, P. Geothermal potential of tunnel infrastructures–development of tools at the city-scale of Basel, Switzerland. *Geothermics* **83,** 101734 (2020).
12. Peltier, M., Rotta Loria, A. F., Lepage, L., Garin, E. & Laloui, L. Numerical investigation of the convection heat transfer driven by airflows in underground tunnels. *Appl. Therm. Eng.* **159,** 113844 (2019).
13. Ogunleye, O., Singh, R. M., Cecinato, F. & Choi, J. C. Effect of intermittent operation on the thermal efficiency of energy tunnels under varying tunnel air temperature. *Renew. Energy* **146,** 2646–2658 (2020).
14. Di Donna, A., Loveridge, F., Piemontese, M. & Barla, M. The role of ground conditions on the heat exchange potential of energy walls. *Geomech. Energy Environ.* 10.1016/j.gete.2020.100199 (2020).
15. Zannin, J., Ferrari, A., Larrey-Lassalle, P. & Laloui, L. Early-stage thermal performance design of thermo-active walls implemented in underground infrastructures. *Geomech. Energy Environ.* 100218 (2020). doi:10.1016/j.gete.2020.100218
16. Bourne-Webb, P., Freitas, T. B. & da Costa Gonçalves, R. Thermal and mechanical aspects of the response of embedded retaining walls used as shallow geothermal heat exchangers. *Energy Build.* **125,** 130–141 (2016).
17. Makasis, N., Narsilio, G. A., Bidarmaghz, A., Johnston, I. W. & Zhong, Y. The importance of boundary conditions on the modelling of energy retaining walls. *Comput. Geotech.* **120,** 103399 (2020).
18. Buhmann, P., Westrich, B., Moormann, C., Bidarmaghz, A. & Narsilio, G. An investigation of the potential thermal energy of geothermal tunnels with focus on a case study in Stuttgart, Germany. in 601–605 (2016).
19. Bidarmaghz, A., Narsilio, G. A., Buhmann, P., Moormann, C. & Westrich, B. Thermal interaction between tunnel ground heat exchangers and borehole heat exchangers. *Geomech. Energy Environ.* **10,** 29–41 (2017).
20. Franzius, J. N. & Pralle, N. Turning segmental tunnels into sources of renewable energy. *Proc. Inst. Civ. Eng.-Civ. Eng.* **164,** 35–40 (2011).

21. Lee, C., Park, S., Won, J., Jeoung, J., Sohn, B. & Choi, H. Evaluation of thermal performance of energy textile installed in Tunnel. *Renew. Energy* **42,** 11–22 (2012).
22. Yosefnejad, D. M., Nagel, T. J. & Froitzheim, N. Three-dimensional modelling of folds, thrusts, and strike-slip faults in the area of Val de Ruz (Jura Mountains, Switzerland). *Swiss J. Geosci.* **110,** 613–630 (2017).
23. Kiraly, L. Notice explicative de la carte hydrogéologique du canton de Neuchâtel. *Neuchâtel Impr. Cent. SA* (1973).
24. Sommaruga, A. Geology of the central Jura and the Molasse basin: new insight into an evaporite-based foreland fold and thrust belt. *Société Neuchâtel. Sci. Nat.* (1997).
25. ISSKA. Avant-projet TransRUN - Synthèse géologique et hydrogéologique 3D. (2011). at <La Chaux-de-Fonds: Unpublished>
26. Bourquin, P., Buxtorf, R., Frei, E., Lüthi, E., Mhlethaler, C., Ryniker, K. & Suter, H. Atlas géologique de la Suisse 1:25'000, feuille 51 Val de Ruz (CN 1144). (1968).
27. Swisstopo. Esquisse hydrogéologique. (2017).
28. SITN. Géoportail du Système d'Information du Territoire Neuchâtelois. (2018).
29. Swiss-Energyscope. Combien la suisse consomme-t-elle d'énergie ? Pour quels usages ? (2018).
30. Office fédéral de la statistique. Ménages. (2017).
31. Etat de Neuchâtel. Population au 31 décembre 2019, Effectifs par commune. (2020).
32. Wilhelm, J. & Rybach, L. The geothermal potential of Swiss Alpine tunnels. *Geothermics* **32,** 557–568 (2003).
33. Frodl, S., Franzius, J. N. & Bartl, T. Design and construction of the tunnel geothermal system in Jenbach. *Geomech. Tunn.* **3,** 658–668 (2010).
34. Nicholson, D. P., Chen, Q., de Silva, M., Winter, A. & Winterling, R. The design of thermal tunnel energy segments for Crossrail, UK. in **167,** 118–134 (Thomas Telford Ltd, 2014).
35. Tinti, F., Boldini, D., Ferrari, M., Lanconelli, M., Kasmaee, S., Bruno, R., Egger, H., Voza, A. & Zurlo, R. Exploitation of geothermal energy using tunnel lining technology in a mountain environment. A feasibility study for the Brenner Base tunnel–BBT. *Tunn. Undergr. Space Technol.* **70,** 182–203 (2017).
36. COMSOL. *COMSOL Multiphysics version 5.5: user's guide and reference manual*. (COMSOL, 2019).

Table 1: Material properties used in the numerical analyses.

Material	**Thermal conductivity, $\boldsymbol{\lambda}$ [$\mathbf{W/(m\,°C)}$]**	**Specific heat, $\boldsymbol{c_p}$ [$\mathbf{J/(kg\,°C)}$]**	**Density, $\boldsymbol{\rho}$ [$\mathbf{kg/m^3}$]**
Soil/rock	Varied (1.5, 2.0, 2.5, 3.0)	1157	1963
Concrete	1.8	880	2300
Water[36]	$= f\,(T)^{*}$	$= f\,(T)^{**}$	$= f\,(T)^{***}$
HDPE pipes	0.35	−	−

* $f\,(T) = -0.869083936 + 0.00894880345 \cdot T - 1.5836634 \cdot 10^{-5} \cdot T^2 + 7.97543259 \cdot 10^{-9} \cdot T^3$

** $f\,(T) = 12010.1471 - 80.4072879 \cdot T + 0.309866854 \cdot T^2 - 5.3818688 \cdot 10^{-4} \cdot T^3 + 3.62536437 \cdot 10^{-7} \cdot T^4$

*** $f\,(T) = 838.466135 + 1.40050603 \cdot T - 0.0030112376 \cdot T^2 + 3.71822313 \cdot 10^{-7} \cdot T^3$

Table 2: Material properties and thermophysical characteristics employed in the numerical simulations of the experimental tests on energy tunnels.

Case study	**Ground temperature, T_{soil} [°C]**	**Ground effective thermal conductivity, λ_{soil} [W/(m °C)]**	**Air temperature, $\overline{T}_a$ [°C]**	**Convection heat transfer coefficient, h_c [W/(m² °C)]**	**Inlet heat carrier fluid temperature, $\overline{T}_{in}$ [°C]**	**Inlet heat carrier fluid velocity $\overline{v}_{in}$ [m/s]**
Jenbach	12	3.0	12 (assumed)	0, 0.5, 1.0 (varied)	2	0.75
Katzenberg	13	3.0	13 (assumed)	0, 0.5, 1.0 (varied)	2	0.75
Seocheon	15	2.5	15 (assumed)	0, 0.5, 1.0 (varied)	33	0.75

669
670 *Table 3: Estimated energy yield achievable through the considered energy tunnel and associated number of households that*
671 *could benefit from its geothermal operation.*

Type of internal airflow	**Extracted thermal power per square meter of energy tunnel**			**Total extracted thermal power from the energy tunnel, [W]**	**Number of households benefitted by**		
	Minimum value, [W/m²]	**Maximum value, [W/m²]**	**Average value, [W/m²]**		**Heating**	**Hot water**	**Heating + hot water**
No airflow, $h_{c1} = 0$ W/(m²°C)	7.45	21.52	13.33	3’659’285	1097	6341	935
Minimal airflow, $h_{c2} = 2.5$ W/(m²°C)	25.35	37.08	30.20	8’590’695	2576	14887	2196
Low-speed airflow, $h_{c3} =$ 12.5 W/(m²°C)	46.86	56.18	50.65	14’564’778	4368	25240	3724
High-speed airflow, $h_{c4} = 25$ W/(m²°C)	53.90	62.49	57.38	16’529’800	4957	28645	4226

672

673

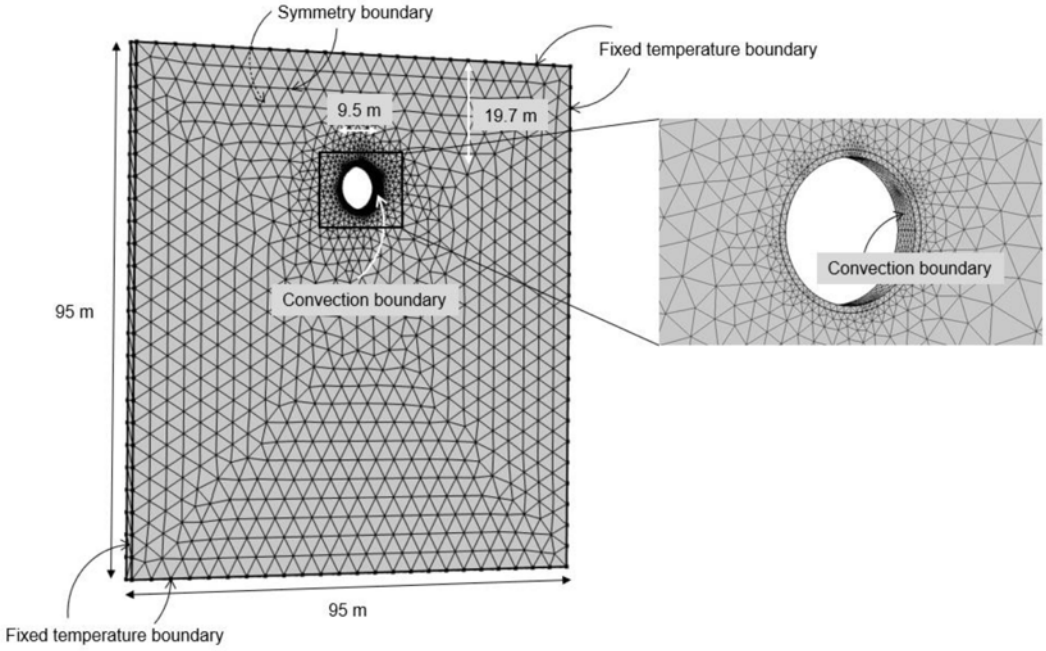

674
675 *Fig. 1: Numerical model employed for the 3-D thermo-hydraulic finite element analyses.*

676

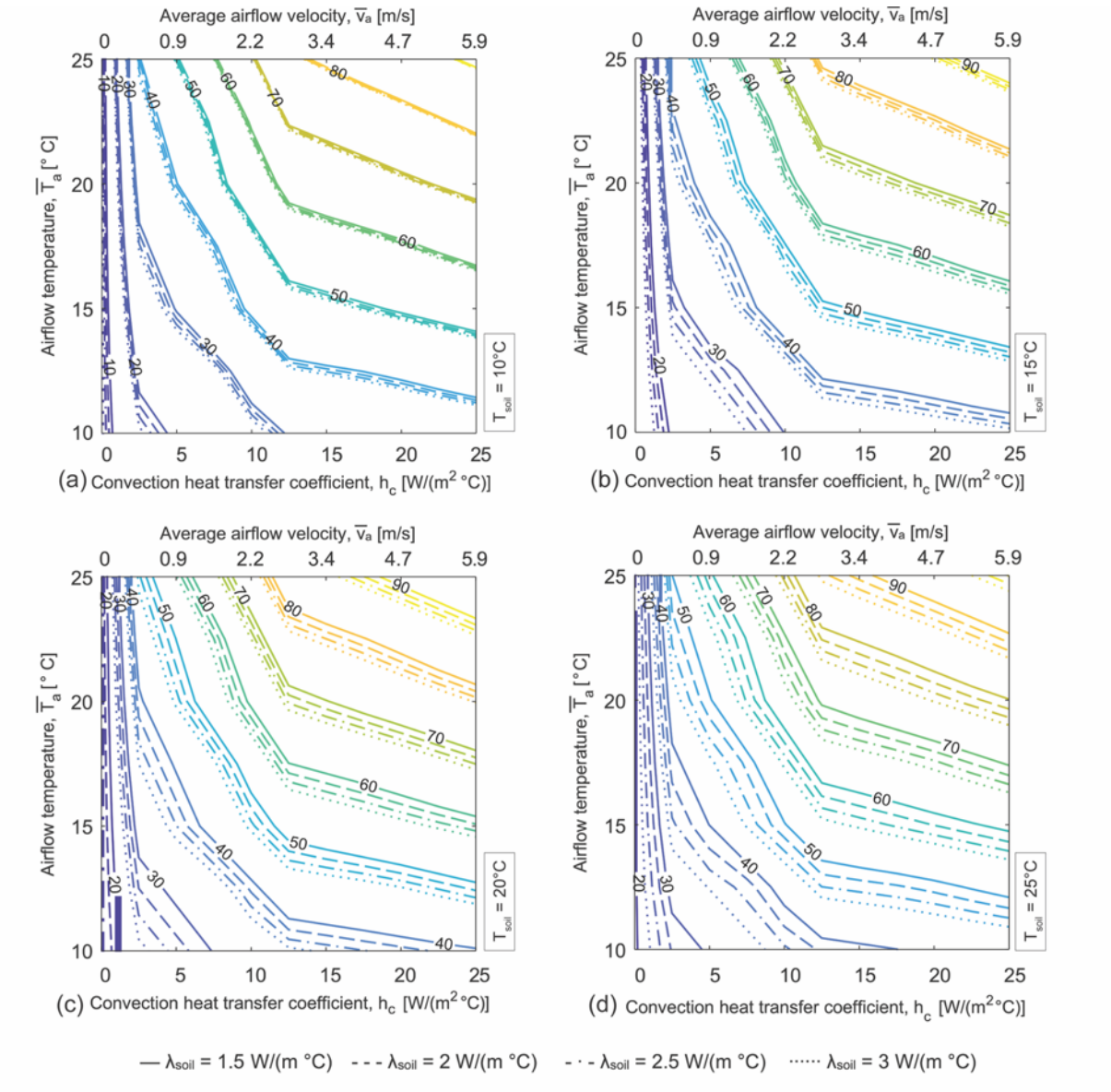

Fig. 2: Extractable thermal power per square meter of thermally active surface of energy tunnels located in geological formations with an undisturbed ground temperature of (a) 10°C, (b) 15°C, (c) 20°C and (d) 25°C.

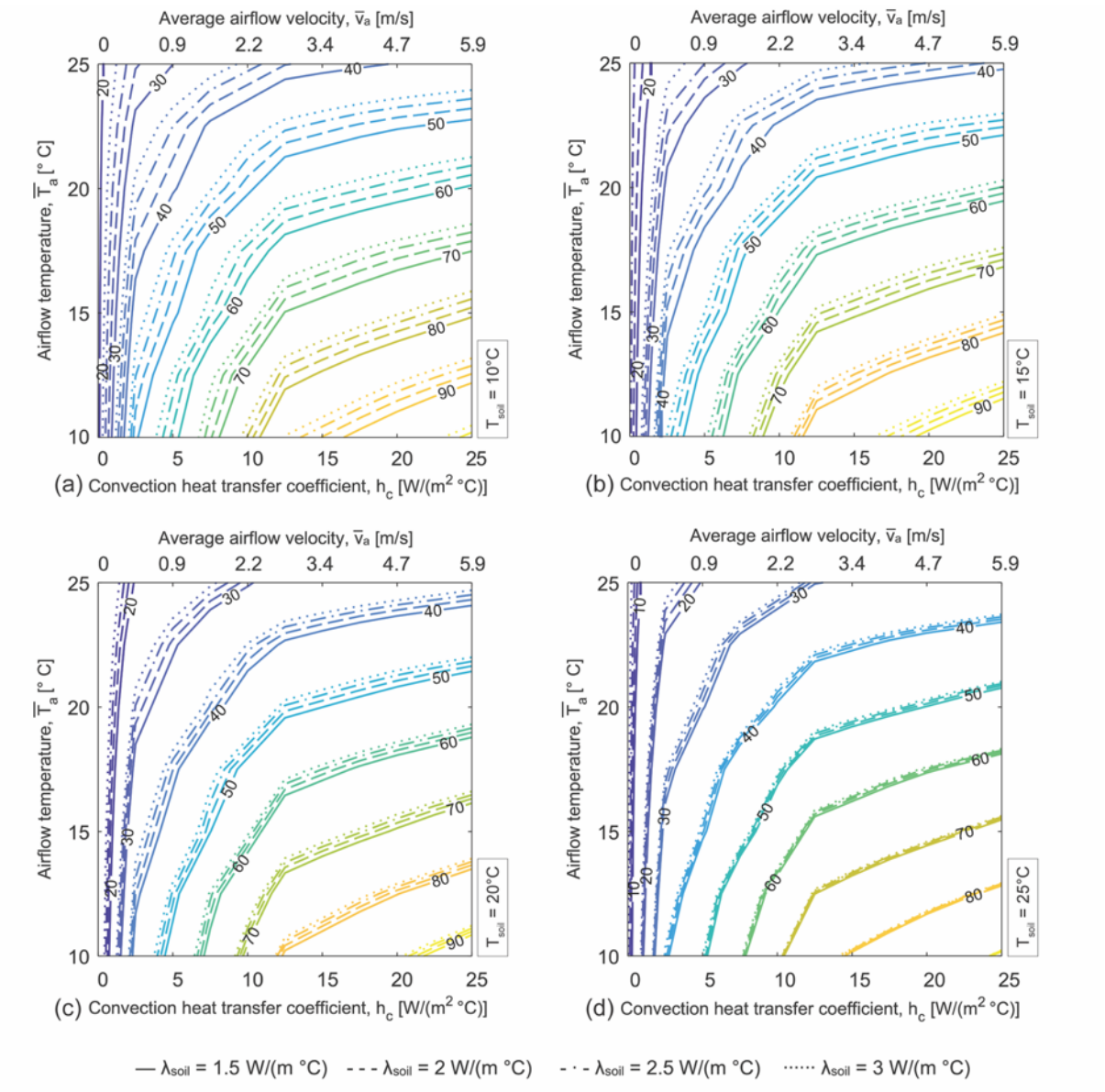

Fig. 3: Injectable thermal power per square meter of thermally active surface of energy tunnels located in geological formations with an undisturbed ground temperature of (a) 10°C, (b) 15°C, (c) 20°C and (d) 25°C.

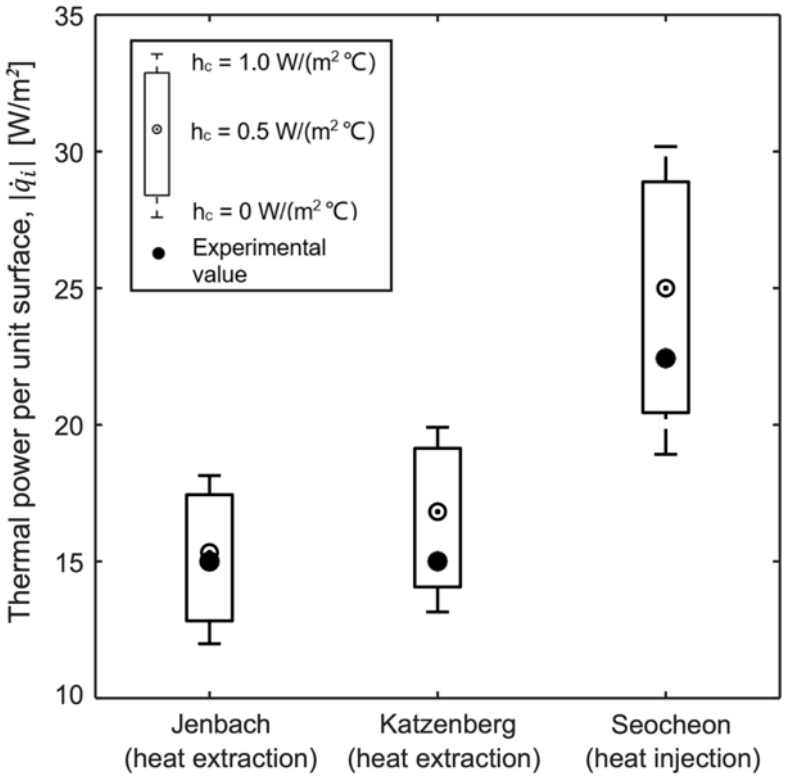

Fig. 4: Experimental validation of the values of thermal power per unit surface provided by the charts presented in this work.

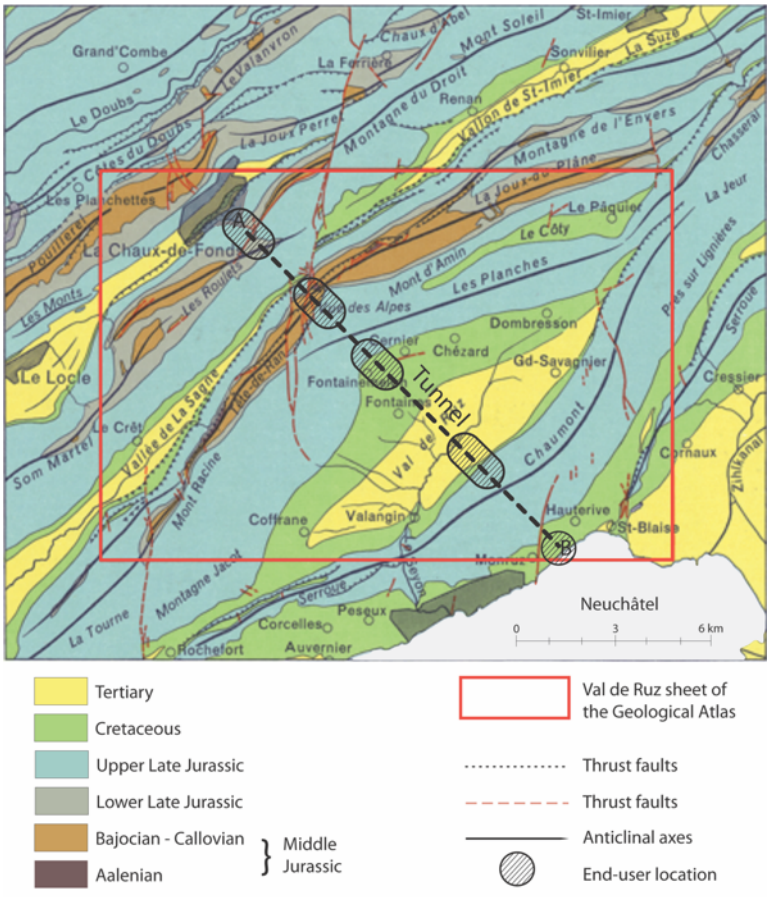

Fig. 5: Plan view of the considered site between Neuchâtel and La Chaux-de-Fonds. The axis of the energy tunnel that is assumed to be constructed in this area is marked with the segment AB. The map and associated legend are adapted from the Geological Atlas GA25 legend[26].

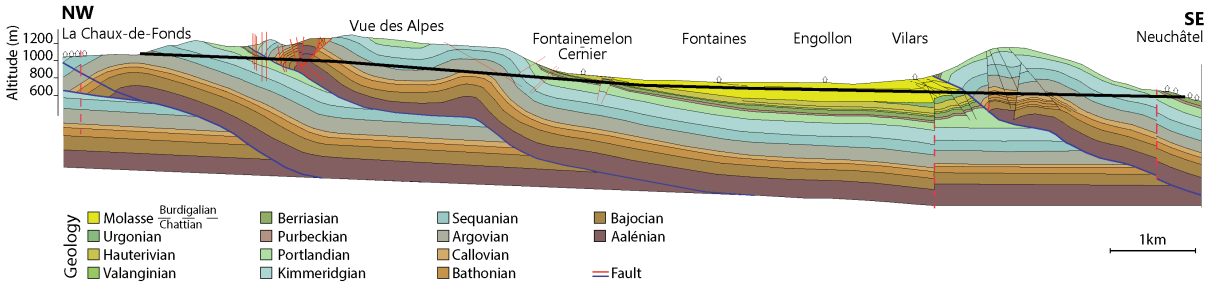

695

696 *Fig. 6: Geological model with the indication of the energy tunnel location (black line spanning from north-west to south-*
697 *east).*

698

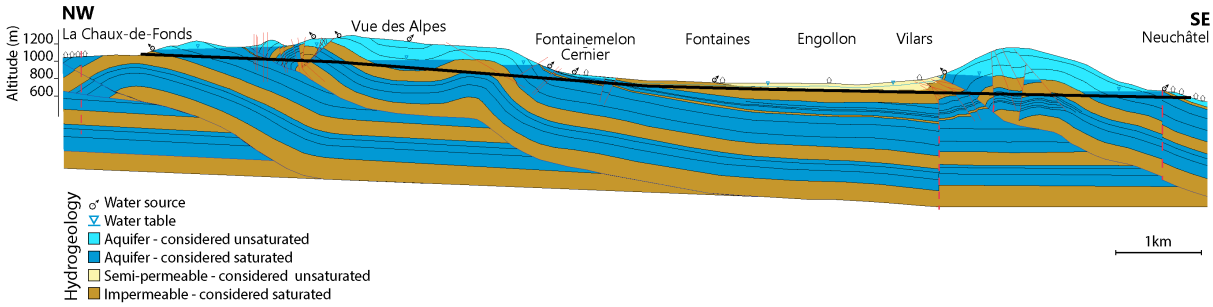

Fig. 7: Hydrogeological model with the indication of the energy tunnel location (black line spanning from north-west to south-east).

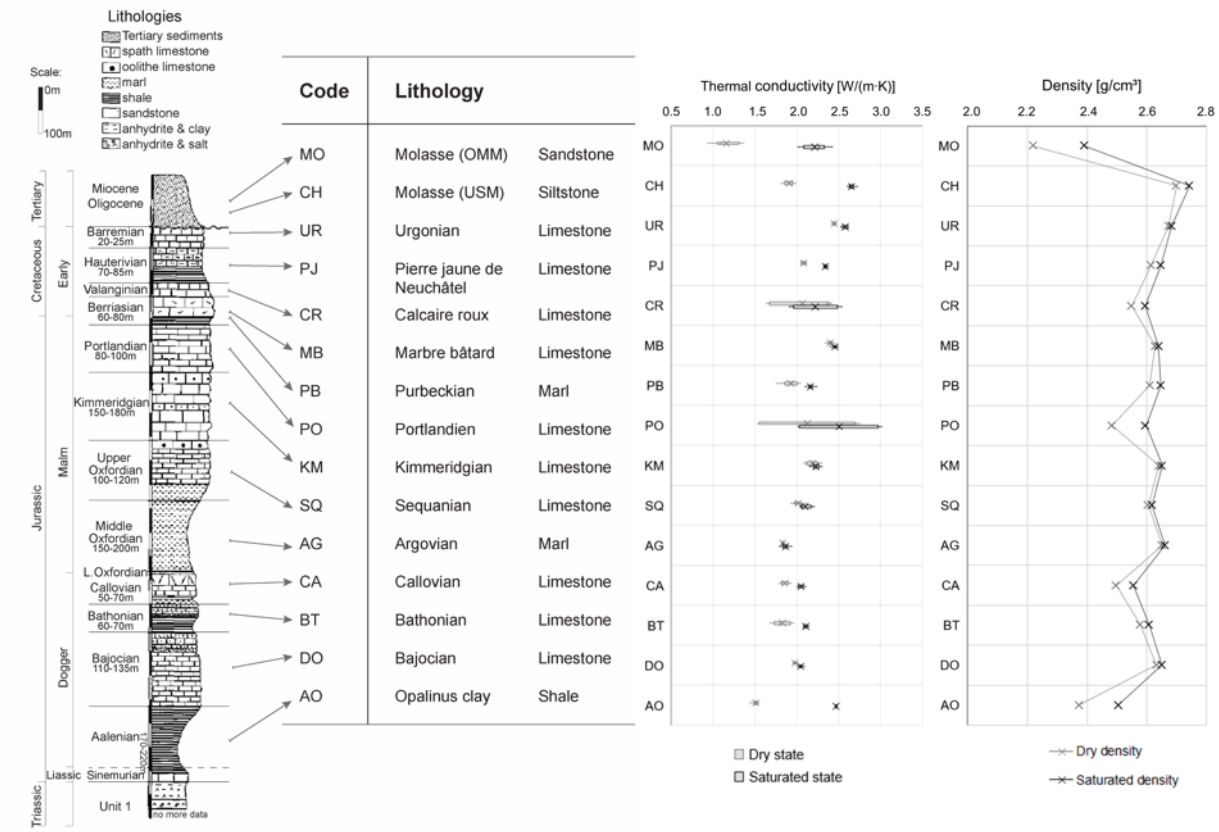

Fig. 8: Thermal conductivity and density results for each lithology, shown in order of the stratigraphic column. For each lithology, thermal conductivity and density were determined in dry (light grey) and in saturated (dark grey) conditions. The graphs represent average values based on experiments done on 2 replicas of each lithology.

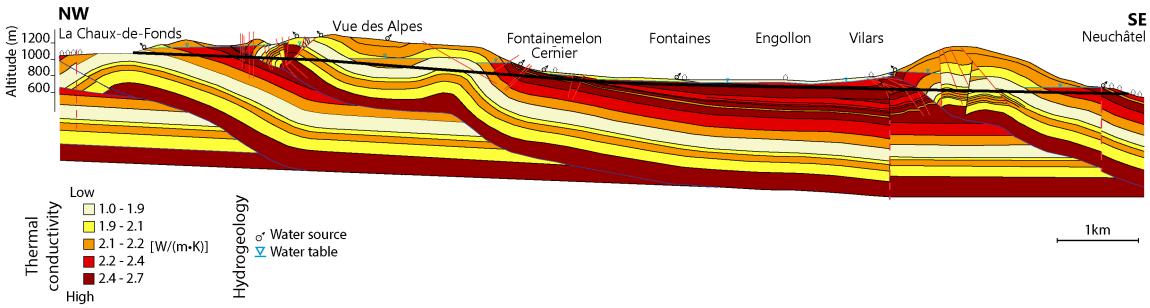

Fig. 9: Thermophysical model with the indication of the energy tunnel location (black line spanning from north-west to south-east).

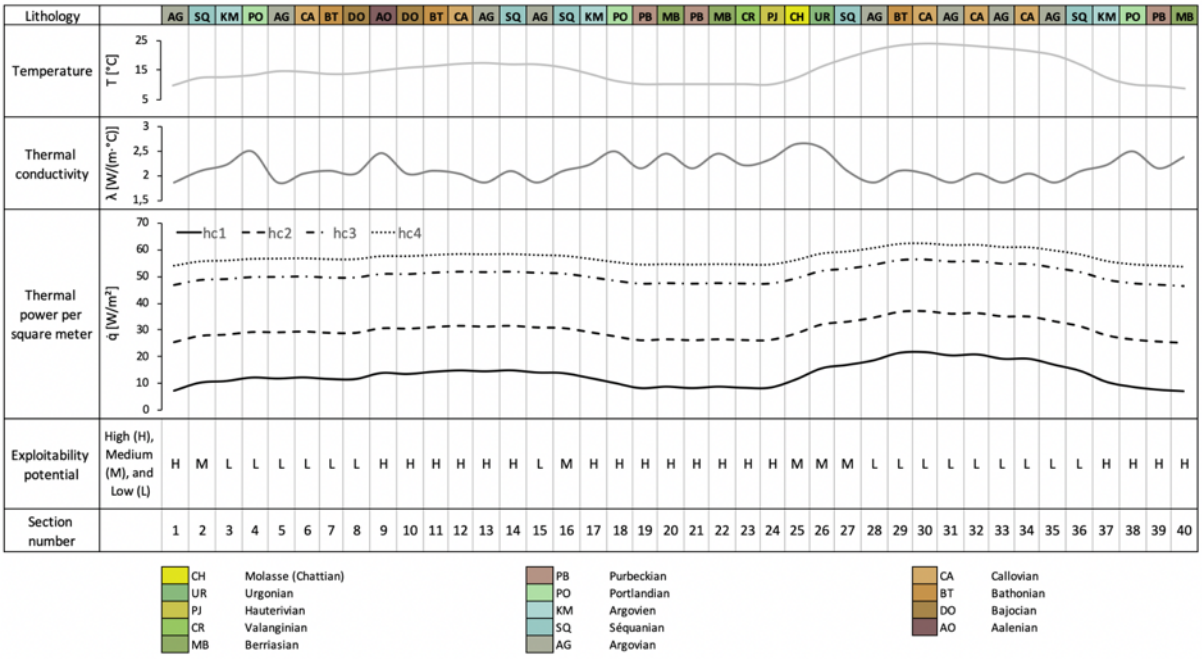

Fig. 10: Estimated thermal power per square meter of each energy tunnel section. The thermal power accounts for the surrounding geological characteristics, including undisturbed ground temperature and effective thermal conductivity, as well as for different internal airflow characteristics. Exploitability potential is assessed based on the distance from the tunnel section to the nearest inhabited areas.